Case Studies in Construction Materials 21 (2024) e03536

Contents lists available at ScienceDirect

Case Studies in Construction Materials

journal homepage: www.elsevier.com/locate/cscm

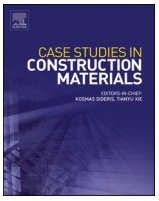

Effect of sodium bicarbonate treatment on the properties of sisal fibers and their geopolymer composites

C. Sanfilippo [a], V. Fiore [a], L. Calabrese [b,*], B. Megna [a], A. Valenza [a]

[a] Department of Engineering, University of Palermo, Viale delle Scienze, Edificio 6, Palermo 90128, Italy
[b] Department of Engineering, University of Messina, Contrada Di Dio (Sant'Agata), Messina 98166, Italy

ARTICLE INFO

Keywords:
Geopolymers
Alkali-activated materials
Composites
Sisal fibers
Sodium bicarbonate treatment

ABSTRACT

Eco-friendly and cheap treatments based on the use of mildly alkaline solutions have been recently investigated to modify natural fibers, altering their surface and improving their compatibility mainly with polymer matrices. A challenge for the researchers is nowadays represented by the assessment of this kind of treatments as a viable approach also for geopolymer based composites. In such a context, this study presents a novel and sustainable approach for enhancing sisal fibers for geopolymer composites using a sodium bicarbonate ($NaHCO_3$) treatment. While the treatment offers a greener alternative to conventional methods, its key advantage lies in achieving a balance between fiber properties. Although it slightly reduces raw fiber strength, the $NaHCO_3$ treatment effectively removes impurities, promoting improved crystallinity and, more importantly, significantly enhances fiber surface roughness and homogeneity. This tailored surface modification fosters superior interfacial bonding with the geopolymer matrix, resulting in composites with significantly enhanced flexural toughness (82 %) – a critical property for construction materials – compared to those reinforced with untreated fibers. Flexural strength is also improved by (53 %). This work not only demonstrates the effectiveness of $NaHCO_3$ treatment but also highlights its potential for developing high-performing, eco-friendly construction materials. A comprehensive evaluation, including three-point bending tests to assess toughness, validates this promising approach.

1. Introduction

Natural fiber-reinforced geopolymer composites have received a huge interest in the last years thanks to their potential to replace traditional cement-based composites. Indeed, geopolymers are well-known for their low energy consumption, low carbon footprint, compressive strength, fire resistance, and long-term durability [1,2]. However, they show quite low tensile and flexural strength values, thus limiting their applicability to semi-structural or non-structural applications [3,4].

To overcome these issues, natural fibers like flax, jute, sisal, coir, and bamboo could be mixed into the geopolymer matrix to increase its toughness capacity [5,6]. The inclusion of fibers in the geopolymer matrix allows increasing the mechanical performances of the composite as well as improving its energy absorption and deformation resistance [7,8]. Geopolymers reinforced with synthetic or natural fiber allow usually to achieve better toughness results in comparison with traditional cement-based composites [8,9]. However, the recent choice is strongly oriented towards the use of natural fibers to increase the environmental sustainability of the

* Corresponding author.
E-mail address: lcalabrese@unime.it (L. Calabrese).

https://doi.org/10.1016/j.cscm.2024.e03536
Received 5 January 2024; Received in revised form 29 May 2024; Accepted 16 July 2024
Available online 18 July 2024

materials.

Natural fiber-reinforced geopolymer composites can be considered as eco-friendly alternatives to traditional cement-based composites and the addition of natural fibers enhances their mechanical properties, making them suitable for various structural applications.

The main concern of the use of natural fiber composites is the relative high moisture absorption of natural fibers, which results in weak compatibility between fibers and the matrix [10,11]. Therefore, modification and functionalization strategies for natural fibers aimed to tailor interface properties and to improve mechanical behavior of cement and geopolymer-based composites become highly important [2,12,13].

Alkaline treatment, a process that exposes the fibers to an alkaline solution, is a common method to improve the performance of natural fibers in concrete composites [14,15]. The alkaline environment disrupts the surface structure of the fibers, removing non-cellulosic components like lignin and hemicellulose and exposing the cellulose microfibrils, which form the primary load-bearing component of the fiber [16]. This treatment enhances the fiber surface area and promotes hydroxyl groups that facilitate chemical bonding with the geopolymer matrix [17].

The enhanced interfacial bonding between fibers and geopolymers leads to substantial improvements in the mechanical properties of geopolymer-based composites. Several studies have reported increased tensile strength, flexural strength and impact resistance, attributed to the enhanced fiber-matrix interaction and improved fiber pull-out behavior [18–20]. Additionally, alkaline treatment can reduce the water absorption and thermal conductivity of composites, further enhancing their performances [14,20,21].

Therefore, alkaline treatment of natural fibers is a crucial step in the development of high-performance geopolymer-based composites. By improving the fiber-matrix interfacial bonding, alkaline treatment enables the synergistic utilization of natural fibers and geopolymers, leading to the production of sustainable, eco-friendly, and high-performance building materials.

While previous studies have explored the use of various treatments to modify sisal fibers for use in composites, a new green approach focused on the application of a mild alkaline treatment with $NaHCO_3$ was suitable applied in natural fiber composites [22]. Sodium bicarbonate represents a cost-effective and eco-friendly alternative to traditional alkaline compounds such as sodium hydroxide for treating natural fibers, widely investigated for thermoset polymer based composites in the last years [23–28]. This approach offers a potentially greener alternative compared to harsher chemical treatments often used. Zamboni Schiavon et al. [29] evaluated impact of chemical treatments on coir fibers, analyzing composition, mechanics, surface chemistry, and morphology. The surface treatment improves fiber properties for potential use in cementitious materials, thus leading to improved physical and mechanical performances of mortars treated coir fibers [30]. Fiore et al. [22] treated sisal fibers with 10 % $NaHCO_3$ solution for 24–240 h, improving tensile strength (197.9 %) and modulus of elasticity (115.0 %) after 120 h. Another study explored sodium bicarbonate as a treatment for sugar palm fibers (SPF) [31]. This treatment resulted in improved thermal stability and crystallinity compared to both untreated and alkali-treated fibers, suggesting potential as a greener alternative for cellulose fiber treatment.

In this concern, this paper presents a novel approach to modifying sisal fibers for geopolymer composites using a sustainable and green surface treatment with sodium bicarbonate ($NaHCO_3$). Unlike traditional methods that often rely on harsh chemicals, this eco-friendly approach investigates the impact of $NaHCO_3$ treatment on fiber properties and, more importantly, its effectiveness in enhancing the flexural strength and toughness of the resulting geopolymer composites. By combining improved fiber performance with a low environmental footprint, this treatment has the potential to become a valuable tool for developing sustainable and high-performing construction materials.

To validate the proposed treatment, a multifaceted evaluation was undertaken, encompassing a comprehensive examination of the chemo-physical and mechanical properties of sisal fibers, complemented by an in-depth assessment of the mechanical performance of the geopolymer composites through three-point bending testing, thus addressing a further improvement of knowledge in the existing literature and providing valuable insights for practical green and sustainable approaches.

2. Experimental part

2.1. Sisal fibers

Sisal plants were extracted from plants collected in a the area near Palermo (Italy), then were washed and dried at 25 °C ± 1 °C for 2 days [22]. The influence of sodium bicarbonate treatment on the properties of sisal fibers was analyzed. To this aim, sisal fibers were soaked at 25 °C for 5 days in $NaHCO_3$ solutions with varying weight concentrations of salt (i.e., 2.5 %, 5 % and 10 % coded as T2.5, T5 and T10, respectively). Afterwards, the treated fibers were washed with distilled water and dried in an oven at 40 °C ± 1 °C for 2 days.

2.1.1. Fourier transform infrared spectrometry

Fourier transform infrared spectrometry (FTIR) was performed on raw and treated sisal fibers by using a Perkin Elmer spectrometer model Spectrum II in order to evaluate the effect of sodium bicarbonate treatment on their chemical components. All the spectra were recorded in attenuated total reflectance (ATR) mode at frequency resolution of 1 cm^{-1} between 500 and 4000 cm^{-1}.

2.1.2. X-ray diffraction

The crystalline phases of raw and treated fibers were determined through an X-ray diffractometer (XRD) by Malvern Panalytical model Empyrean, operating at 40 kV and 30 mA. A 2-theta scan from 6° to 40º with a step size of 0.026° was assessed by using the monochromatic radiation from CuKα with wavelength $\lambda = 0.154$ nm.

The crystallinity index (CI) of sisal fibers was calculated by using Segal empirical equation [x]:

$$CI(\%) = \frac{I_{200} - I_{am}}{I_{200}} \times 100$$

I_{200} represents the maximum intensity of the crystalline phase (i.e., the 200 lattice planes) peak at 2θ angle equal to 22.6° whereas I_{am} denotes the intensity of the amorphous phase present in the fiber, calculated as the height of the valley of the minimum between the (220) and (110) peaks.

2.1.3. Tensile tests

50 samples were tested in tensile configuration for each investigated condition. In particular, all tensile tests were carried out in accordance with the ASTM D 3379 standard, by using a U.T.M. by Zwich- Roell model Z005, equipped with a 200 N load cell. The gage length and the strain rate were set equal to 70 mm and 1 mm/min, respectively. The experimental data were then statistically analyzed using a two-parameter Weibull distribution.

2.1.4. Thermogravimetric analysis

Thermogravimetric analysis (TGA) was carried out to investigate the thermal behavior of sisal fibers with the aid of a thermo-balance model STA Model f1 Jupiter by Netzsch. Samples of untreated and treated fibers (20–30 mg) were heated from 30 °C to 1000 °C at a heating rate of 10 °C/min in nitrogen atmosphere.

2.2. Geopolymer composites

Geopolymer composites were manufactured by using a metakaoline (Silicon to Aluminum molar ratio of 1.3:1; grain size distribution in the range 1 μm - 100 μm) as precursor, which was activated through a 7 M water solution of potassium hydroxide (KOH). All geopolymer samples were made by setting the metakaoline to alkaline activator ratio equal to 1:1. In particular, the process began by mixing metakaoline with potassium silicate powder ($K_2O{\cdot}nSiO_2$) in combination with river sand following a specific mix ratio of 1:0.5:2. Subsequently, KOH solution was added to the mixture, to allow the geopolymerization process. To enhance the composite's properties and their sustainability, 2 wt% of the aggregate was replaced with raw and treated sisal fibers, with a nominal length of 2.5 mm. Natural fibers were soaked in $NaHCO_3$ solutions at varying the weight concentration (i.e., 2.5, 5 and 10 %) for 5 days at room temperature.

The following codes were used in this study to indicate the geopolymer composites: MK-T0, MK-T2.5, MK-T5 and MK-T10. For instance, MK-T10 indicates sisal fibers used to reinforce the geopolymeric matrix have been previously treated in 10 % $NaHCO_3$ solution.

2.3. Three-point bending tests

Prismatic samples (40 mm×40 mm x 160 mm) were tested under three-point bending loading, by using a universal testing machine ETM-C (WANCE, Shenzhen China), equipped with a 50 kN load cell. The span length was set equal to 100 mm and a pre-load of 10 N

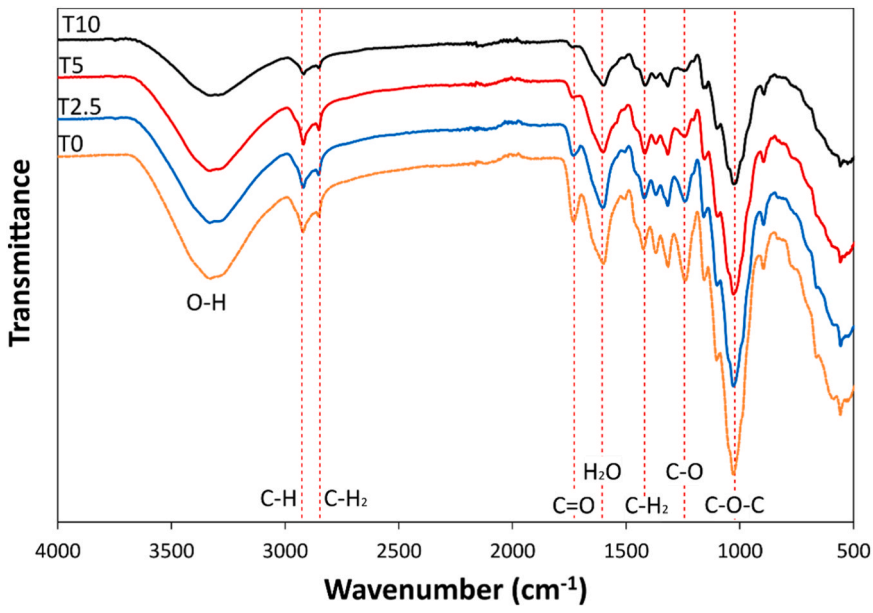

Fig. 1. FT-IR spectra of untreated and treated sisal fibers.

was applied at the beginning of each test to stabilize the testing fixture. All the quasi-static tests were carried out in displacement control setting the rate equal to 1 mm/min rate, according to EN 1015–11 standard. Five specimens were tested for each condition investigated.

The fracture surface features of geopolymer composites and treated and untreated natural fibers were examined using a FEI Quanta 600 ESEM microscope operating at 20 kilovolts. To prevent electrostatic charging during the scanning electron microscopy (SEM) analysis, all specimens were coated with a thin layer of gold.

3. Results and discussion

3.1. Sisal fibers

3.1.1. Functional groups analysis

With the purpose of evaluating the functional groups modification induced by the mildly alkaline treatment, Fig. 1 compares the FTIR spectra of sisal fibers treated at varying $NaHCO_3$ concentration (i.e., T2.5, T5 and T10, respectively) and untreated fibers (i.e., T0) as reference.

The spectrum of untreated sisal fiber (i.e., T0 batch) allows emphasizing the most important transmittance peaks, which characterize the natural fiber. Starting from high wavelengths, the wide peak with a maximum at 3330 cm^{-1} can be attributed to the O-H stretching vibration and hydrogen bond of the hydroxyl groups [32]. The two peaks at 2922 cm^{-1} and 2853 cm^{-1} are indicative of the C-H stretching vibration (methylene CH_2, and aliphatic saturated CH, respectively) in cellulosic and hemicellulose molecules [33]. Instead, the stretching vibration of the C═O carbonyl group binding the carboxylic acid in lignin or the ester group in hemicellulose is responsible for the appearance of a broad and distinct absorption band centered at 1726 cm^{-1} [34]. Furthermore, this peak can be ascribed to pectin and waxes scattered in the sisal fiber, according to [35].

The broad and relevant peak centered at 1596 cm^{-1} can be associated to the presence of water in the lignocellulosic fibers [36], while the smaller peak at 1503 cm^{-1} is caused by the C═C stretching of the functional group of alkenes (i.e., lignin) [37]. The absorbance at 1424 cm^{-1} is due to the symmetric bending of CH_2 in cellulose, hemicellulose and lignin [38], whereas the absorbance peaks at 1367 cm^{-1} and 1314 cm^{-1} can be ascribed to the bending vibration of the C-H and C-O groups of the aromatic ring in polysaccharides [39]. The C-O stretching vibration of the acetyl group in lignin is responsible for the absorbance peak at 1241 cm^{-1} [40]. Additionally, two extremely bright peaks can be observed at 1105 cm^{-1} and 1029 cm^{-1}, which can be associated with the stretching vibration of the C-O-C of the pyranose ring in the polysaccharides [41] and hydroxyl and ether groups in cellulose [42]. The peak at 897 cm^{-1} is attributed to the presence of b-glycosidic linkages between the monosaccharides [43].

The impacts of $NaHCO_3$ treatment on sisal fiber surfaces were likewise assessed by FTIR spectra modifications (as shown in Fig. 1). In order to compare all transmittance spectra, the FTIR peaks are baseline corrected to the peak at 3330 cm^{-1}. From the comparison, it is possible to observe that the signal at 1730 cm^{-1}, attributable to the carbonylic group C═O stretching vibration of carboxylic acid linkage in lignin or ester group in hemicellulose, waxes and oils, is not observable in the spectra of treated fibers, regardless of the solution concentration. These considerations disclose that the $NaHCO_3$ treatment allows the partial removal of hemicellulose from the fiber surface [22,44] and waxes may be partially decomposed during the process, thus directly affecting the surface characteristics of the fiber itself [45].

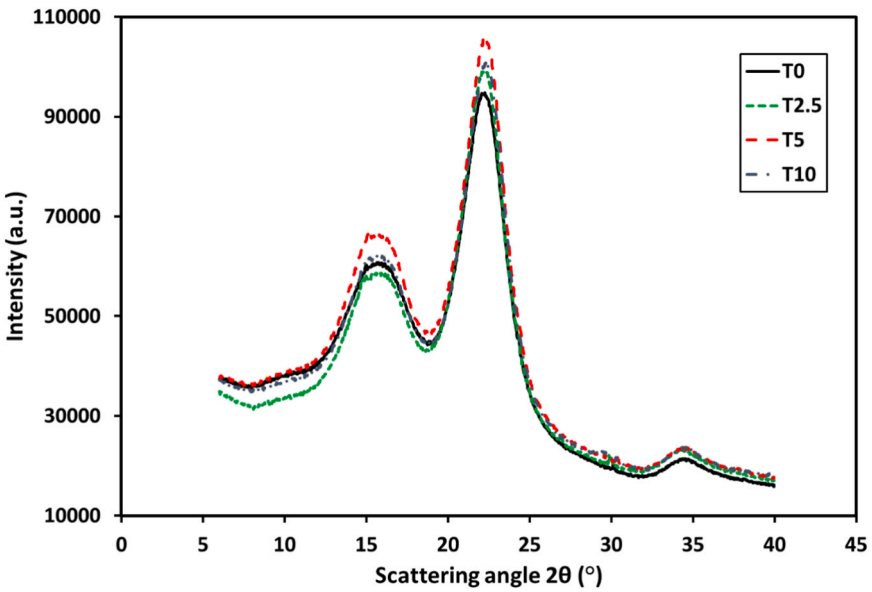

Fig. 2. XRD patterns of untreated and treated sisal fibers.

Furthermore, the peak centered at 1241 cm^{-1} is less visible for treated fibers than for untreated ones. As mentioned above, this peak can be ascribed to the C-O stretch of the acetyl group of lignin, and it is lowered because lignin is partly removed from the fiber surface [46]. Overall, the main effects of the mildly alkaline treatment in sisal natural fibers consist in the removal of hemicellulose as well as the decrease of lignin content from sisal fibers.

The removal of these compounds as well as of impurities, wax and fatty substances from the fiber surface leads to fibrillation and consequent reduction of fibers diameter, thus increasing their aspect ratio. Furthermore, the mechanism of action of alkaline treatment consists in the disruption of hydrogen bonds on the fiber surface, thereby increasing its roughness [47]

All these effects contribute to make natural fibers more compatible with hydrophobic polymers: i.e., the enhanced chemical and mechanical compatibility strengthens the interfacial fiber-matrix bonding, thus leading to significant enhancements in the mechanical properties of the composites.

3.1.2. Crystalline structure observation

The XRD patterns of raw and treated fibers are illustrated in Fig. 2.

The X-ray diffraction (XRD) analysis revealed a prominent and distinct crystalline peak for the sisal fiber, corresponding to the crystallographic planes (200) and (110) of the cellulose, at high (i.e., ~22°) and low (i.e., ~16°) scattering angles, respectively. Interestingly, after subjecting the fiber to the mildly alkaline treatment, the position of the (200) peak slightly shifted towards higher angles. This shift indicates a soft reduction in the interplanar spacing of the (200) planes [48].

The findings of the study indicate that the treatment using low concentrated solution leads to an enhancement in the (200) peak intensity. This increase suggests a higher level of crystallinity in the modified fibers. It is proposed that this improvement in crystallinity may be attributed to the rearrangement of cellulose molecules following the removal of substances such as hemicellulose, lignin, pectin, and others through various treatments [49], in accordance with FTIR results.

When sisal fibers are treated with an alkaline solution, the alkali molecules attack the amorphous components of the fibers, namely hemicelluloses and lignin. These amorphous components are responsible for the surface roughness and hydrophilic nature of the fibers, which can hinder their adhesion to polymer matrices [50].

By removing these amorphous components, the mildly alkaline treatment exposes the crystalline cellulose, which is hydrophobic and has better bonding properties. Furthermore, this removal of amorphous components leads to an increase in the fibers crystallinity, as more of the fiber's structure is organized into crystalline regions.

However, these findings clearly indicate that the chosen treatment conditions are suitable to avoid the triggering of crystalline cellulose degradation phenomena. Indeed, a too aggressive alkaline environment can lead to unwanted decreases in the overall crystallinity of the fiber itself [51], mainly due to the hydrolysis of cellulose chains, which breaks them into smaller fragments [52].

To confirm these statements, the empirical Segal equation was used to calculate the reported crystallinity index (CI) values for all samples, as shown in Table 1. it can be observed that the eco-friendly treated fibers have CI of about 3 % higher than untreated one.

3.1.3. Morphological analysis

Fig. 3 compares the SEM images at different magnifications of raw and treated sisal fibers.

By analyzing Fig. 3a), it can be observed that untreated fibers are characterized by cellulose microfibrils, oriented longitudinally in parallel alignments, bound together through a layer of hemicellulose, lignin and waxes. On the other hand, treated sisal fibers showed different surface appearance: i.e., the increase in the concentration of the alkali solution determines a progressive surface deterioration of the fiber, which modifies its morphology.

Fig. 3b) evidences that slight fiber deterioration is observable when it is soaked in less concentrated solution (i.e., T2.5 batch). The removal of some surface constituents, such as waxes, cuticles and globular particles, generates some pits on the fiber surface with the beginning of the formation of grooves takes place [53]. However, the surface is still quite smooth, very similar to that of untreated fibers: i.e., it can be assumed that the treatment condition was not suitable to induce significant surface modifications.

As clearly shown in Fig. 3c), by increasing the solution concentration to 5 wt% (i.e., T5 batch), the fiber surface degradation begins to become noteworthy. In particular, the protective layers of lignin and hemicellulose were at least partially destroyed, as evidenced by the fibrils separation and the exposure of the helical structure of cellulose microfibrils, made of square-shaped spirals. This partial degradation of the lignin and hemicellulose matrix resulted in a rougher surface, which can improve the available contact area and adhesion between the fiber and the geopolymer matrix.

Finally, Fig. 3d), which shows the longitudinal view of sisal fiber treated in 10 wt% $NaHCO_3$ solution (i.e., T10 batch), highlights that the fibrillation is further increased. However, the onset of superficial damage of the fiber itself is also observed. In particular, damage or stripping of the microfibrils can be noticed, due to the partial removal of non-cellulosic materials from the external layer.

Table 1
Crystallinity index values of untreated and treated sisal fibers.

	Crystallinity Index [%]
T0	53.4
T2.5	56.7
T5	56.1
T10	56.2

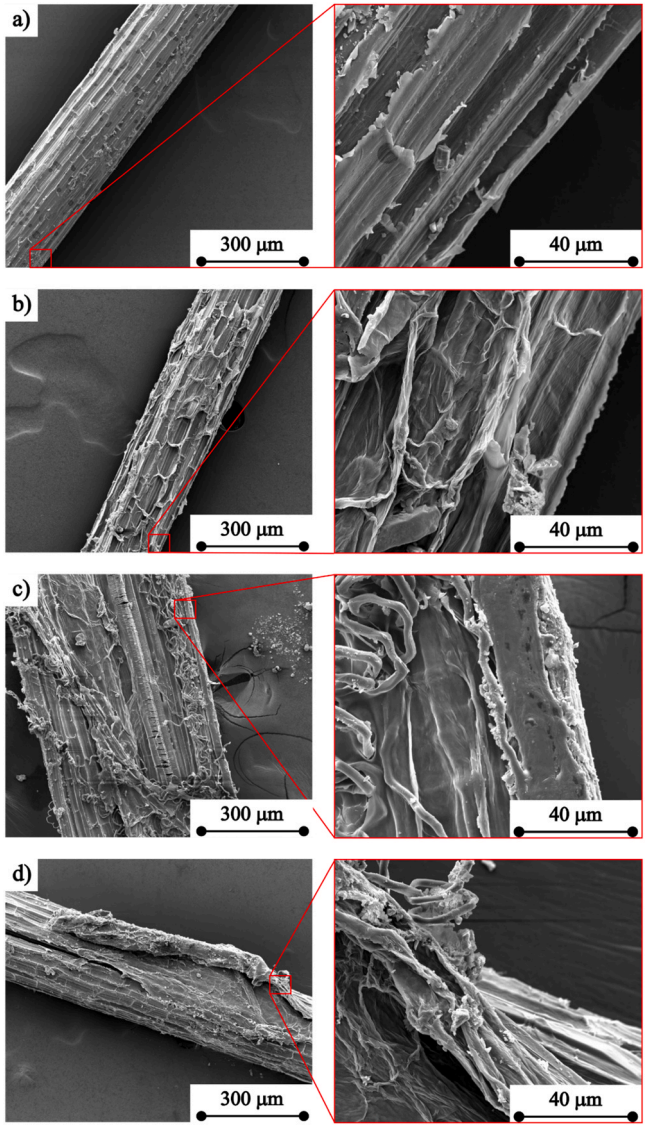

Fig. 3. Morphological images of a) T0, b) T2.5, c) T5 and d) T10 fibers.

This reveals the internal cellulosic microfibrils thus contributing to the fibrils separation.

Overall, the degradative action of the alkaline treatment consists of different phases, whose kinetics are strictly related to the exposure time and to the aggressiveness of the solution. The first step brings to the degradation of lignin and part of the hemicellulose content, followed by stripping of cellulose microfibrils and then by alkaline hydrolysis of the amorphous regions of the cellulose.

Therefore, the inadequate choice of treatment conditions such as immersion time or concentration of the solution can imply the activation and evolution of significant and irreversible degradation phenomena on the natural fiber. This could have a harmful effect on the mechanical performances of the fiber and represents a warning to pay attention in order to define a threshold value for the fiber treatment to be applied.

3.1.4. Single-filament tensile tests

By observing the typical stress-strain curves shown in Fig. 4, it can be observed that, regardless of the treatment condition, sisal fibers exhibit mainly brittle behavior with a sudden and relevant load drop at first crack triggering. Although, the analysis of the single filament tensile test was difficult cause of the high scatter of the data. Indeed, by considering the wide chemical-physical variability of natural fibers as well as their structural and geometric intrinsic heterogeneity, it is widely known that the mechanical properties of the fibers are highly scattered and characterized by a wide dispersion of data [54,55]. Furthermore, this distribution is also related to anthropic characteristics (difficult to be parameterized) such as soil conditions, extraction or drying process. Consequently, the application of statistical approaches (such as Weibull distribution) represents a potentially effective strategy for specifically evaluating

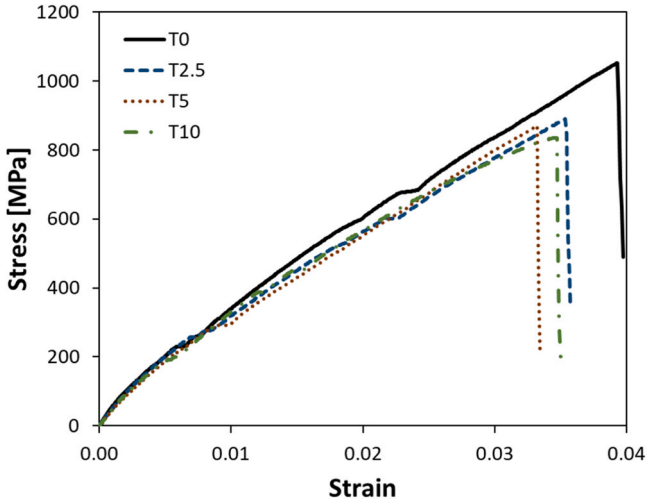

Fig. 4. Typical tensile stress versus strain curves of untreated and treated sisal fibers.

the test results and being able to better correlate the results acquired from different batches of treated and untreated fibers [56].

In such a context, Fig. 5 compares the Weibull distributions of the tensile strength of raw and treated sisal fibers, showing the plots of ln/-ln(1-F(σ))) versus ln(σ) with a least square fit for the best fitting line. The Weibull model was applied on all batched exhibiting a good fitting of the experimental data, regardless of the treatment condition, meaning that the Weibull distribution offers a reasonable approximation of the tensile strength.

Fig. 5 presents the statistical characteristics of tensile strength for raw and treated fibers. It is evident that the tensile strength decreases with increasing the concentration of the $NaHCO_3$ solution. In particular, T10 batch exhibited a reduction of the scale parameter of 17.4 % in comparison to untreated fibers (i.e., T0 batch).

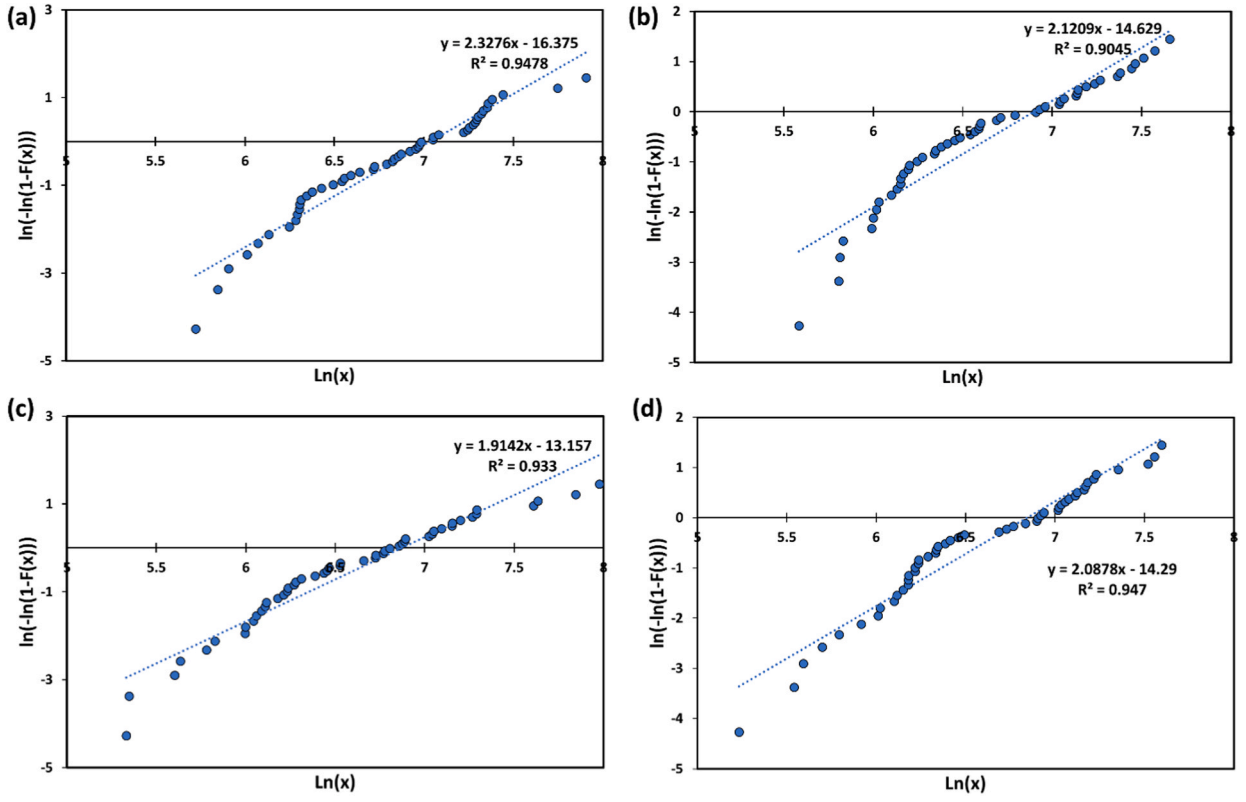

Fig. 5. Weibull distribution of tensile strength (x) for a) T0, b) T2.5, c) T5 and d) T10 fibers.

This can be partially attributed to the modifications induced in the chemical composition of sisal fibers after the soaking in the $NaHCO_3$ solutions, which effectively removed the non-cellulosic components such as hemicelluloses and lignin, as clearly revealed by FTIR analysis.

Furthermore, the mildly alkaline treatment causes detrimental effect on the fiber morphology that evidences the presence of some pits on the surface with the consequent formation of evident grooves. As shown by SEM images, these morphological modifications are more evident with increasing the alkalinity of the sodium bicarbonate solution.

All these effects induced by the proposed treatment can help us to explain the slight average reduction in the tensile strength experienced by treated sisal fibers in comparison to untreated ones.

The scale parameter (or spread, η) is related to the mean stress at failure. It is defined in Weibull analysis as the stress at which 63.2 % of the fibers under consideration broke. By evaluating in detail the data reported in Table 2, it is possible to notice that the trend of this parameter is in accordance with that of the mean value.

On the other hand, the shape parameter (or Weibull modulus) can be used to evaluate the surface integrity of the treated surface. The higher the shape parameter, the narrower the distribution of the fiber strength values. For natural fibers, which are characterized by large data dispersion, the Weibull modulus is usually ranging between 1 and 6 [48]. For raw and treated sisal fibers investigated in the present work, the calculated shape parameter ranges between 1.9 and 2.3, compatible with other natural fibers.

Furthermore, the interquartile range (i.e., IQR parameter in Table 2) is related to the spread of the middle half of the failure stress distribution of the fibers. It is calculated as the difference between the upper Q3 and lower Q1 quartiles, hence it identifies the width of the range of values that contains the middle-half of the data. It was found that this parameter decreases by increasing the solution concentration.

This confirms that the distribution of the stress at failure values is more compact more concentrated towards the peak value of the bell-shaped distribution of data.

This finding, as also confirmed by the standard deviation values, indicates that treated fibers are more homogeneous and therefore characterized by a lower dispersion of their mechanical performance compared to raw ones.

With the aim of better evaluating the statistical peculiarities related to the fiber failure values, the cumulative probability function of the tensile strength of treated and untreated fibers is shown in Fig. 6. The evolution of the cumulative probability function related to untreated fibers (i.e., T0 batch) is shifted toward higher values than those of treated ones, thus confirming that the surface treatment led to a reduction of the stress at failure of sisal fibers. At the same time, a slight increase of the curve slope can be also identified (i.e., more evident for T10 batch), ascribed to a narrow dispersion of the data around the average value.

A fitting with a two parameter Griffith's model was also done to assess the evolution of the tensile strength (σ) as a function of fiber diameter (d) for all the investigated fiber batches. In particular, the Griffith empirical model relates the variation of the mechanical performance with the fiber diameter according to the following expression:

$$\boldsymbol{\sigma}(\boldsymbol{d}) = \boldsymbol{A} + \left(\frac{\boldsymbol{B}}{\boldsymbol{d}}\right) \tag{1}$$

Where A and B are two fitting constants.

As shown in Fig. 7, the superimposed dotted red lines (drawn applying the Griffith model) reveal a decrease in the fiber strength at increasing the diameter. This is justified by considering that natural fibers with large cross-sectional area show an higher number of flaws and defects than fibers having smaller cross-sectional area [57]. Furthermore, it can be observed that there is a good agreement between the Griffith curves and the experimental data, indicating that the model can suitably predict the mechanical characteristics' dependency with the fiber size.

However, a greater dispersion in the distribution of the tensile strength values as function of fiber diameter can be identifiable for the T2.5 batch, in comparison to the other batches of fibers treated in higher concentrated sodium bicarbonate solutions (i.e., T5 and T10 batches). This result can be ascribed to the use of a non-effectively aggressive alkaline solution: i.e., it doesn't allow an adequate surface cleaning of the fiber thus achieving only locally the dissolution of the surface waxes, hemicellulose and lignin, as already evidenced by SEM images. The consequence is a not effective correlation between the failure tensile strength and fiber diameter, whereas T5 and T10 batches evidenced a good experimental correspondence between these two parameters.

Table 2
Characteristic statistical parameters for tensile strength of untreated and treated sisal fibers.

	Tensile Stress			
	T0	T2.5	T5	T10
Scale Parameter [MPa]	1136.2	989.8	966.3	938.6
Shape Parameter	2.3	2.1	1.9	2.1
Mean Value [MPa]	1010.3	879.8	869.8	834.4
Standard Deviation [MPa]	509.0	488.1	479.0	454.6
Median [MPa]	939.3	718.7	683.0	649.3
IQR	835.5	752.5	677.5	671.1
Correlation	0.95	0.90	0.93	0.95

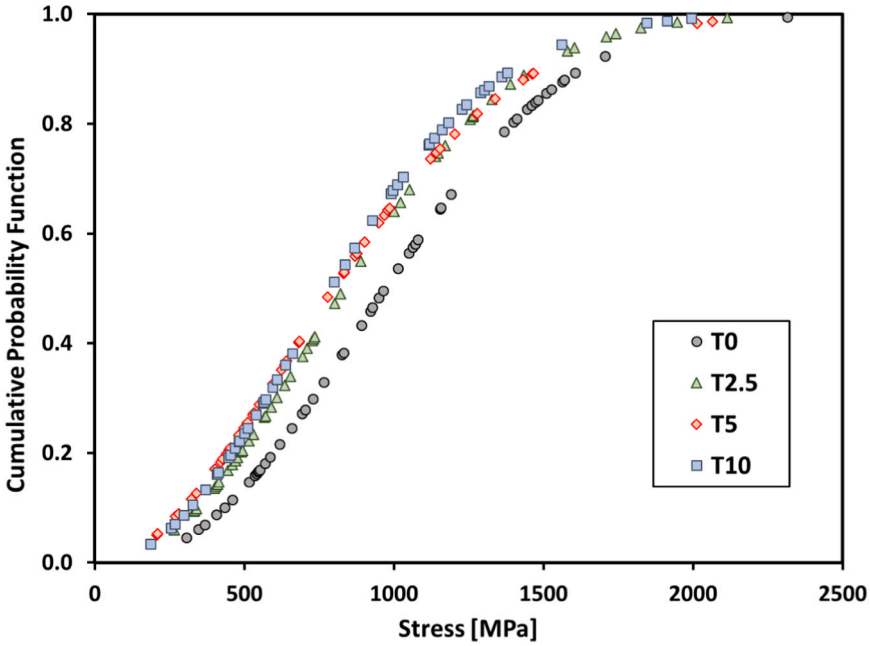

Fig. 6. Cumulative probability function of tensile strength for treated and untreated sisal fibers.

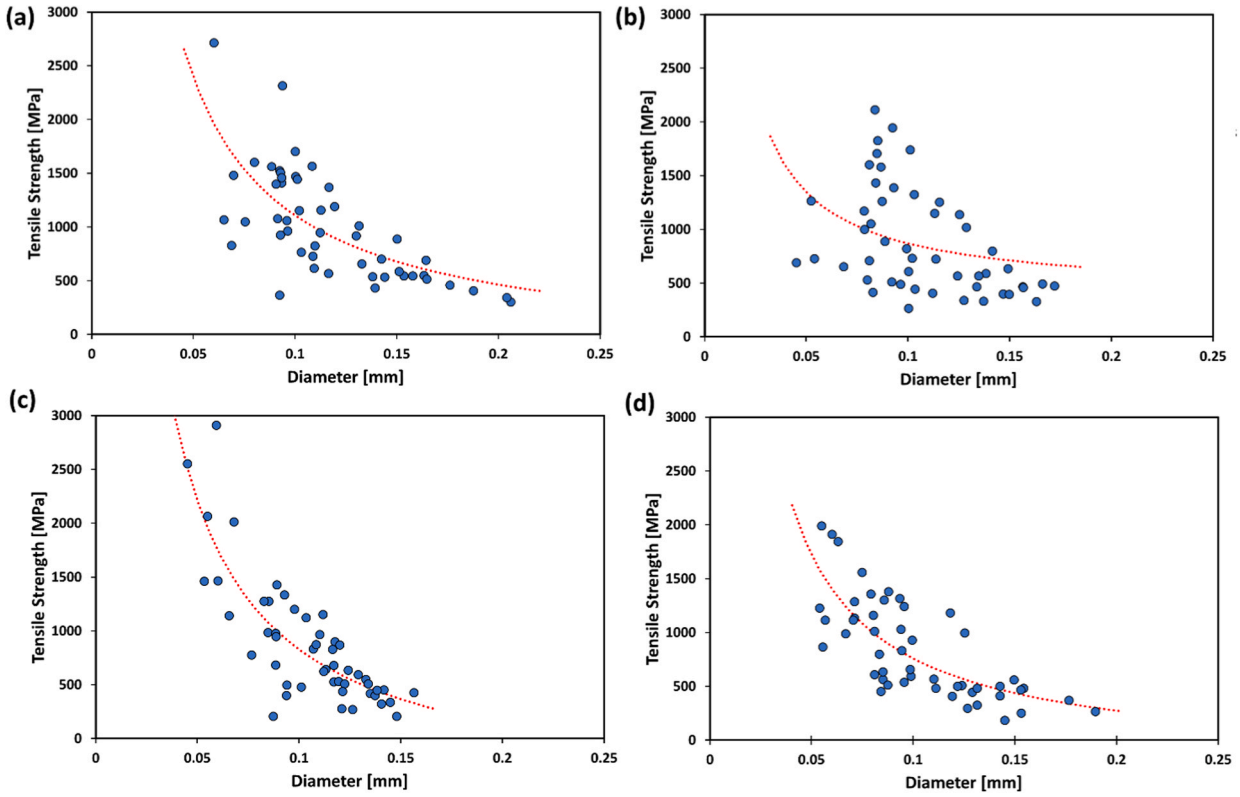

Fig. 7. Experimental data and Griffith model (i.e., dotted line) for tensile strength for a) T0, b) T2.5, c) T5 and d) T10 fibers.

3.1.5. Thermal stability

Fig. 8 shows the results of the thermogravimetric analysis performed on untreated and treated sisal fibers.

Both figures clearly evidence that untreated and treated fibers show a first peak due to the water evaporation in the range 30 °C -

150 °C. In this temperature range the loss in weight was about 9.3 %, 7.2 %, 7.5 % and 8.4 %, for T0, T2.5, T5 and T10, respectively. This confirms the reduction of the fiber hydrophilicity after the mildly alkaline treatment.

Afterwards, all the curves (i.e., regardless the treatment condition) shows two thermal degradation phases. In particular, the onset degradation temperature of all sisal fibers is about 250 °C and the first degradation peak, caused by the depolymerization of hemicelluloses and pectin and the glycosidic linkages of cellulose, is centered in the range about 290 °C-300 °C for all the investigated fibers. This peak is clearly observable in the DTG curve of untreated fibers whereas it tends to disappear for treated fibers. During this degradative step, it is worth noting that the weight losses experienced by T0, T2.5, T5 and T10 samples were equal to 39.4 %, 36.4 %, 35.8 % and 37.2 %, respectively. These findings are in accordance with the results of FTIR, which clearly showed the reduction of hemicellulose content due to the soaking of sisal fibers in $NaHCO_3$ solutions.

Finally, the degradation of α-cellulose can be noticed by observing the final peak between 335 °C and 348 °C for all the investigated fibers. No specific peak can be attributed to the lignin degradation, because this component is characterized by a complex structure of aromatic rings with various branches. Hence, its degradation occurs slowly in the entire temperature range.

Overall, the thermal analysis confirms that, similarly to mercerization, the mildly alkaline treatment allows to partially remove the

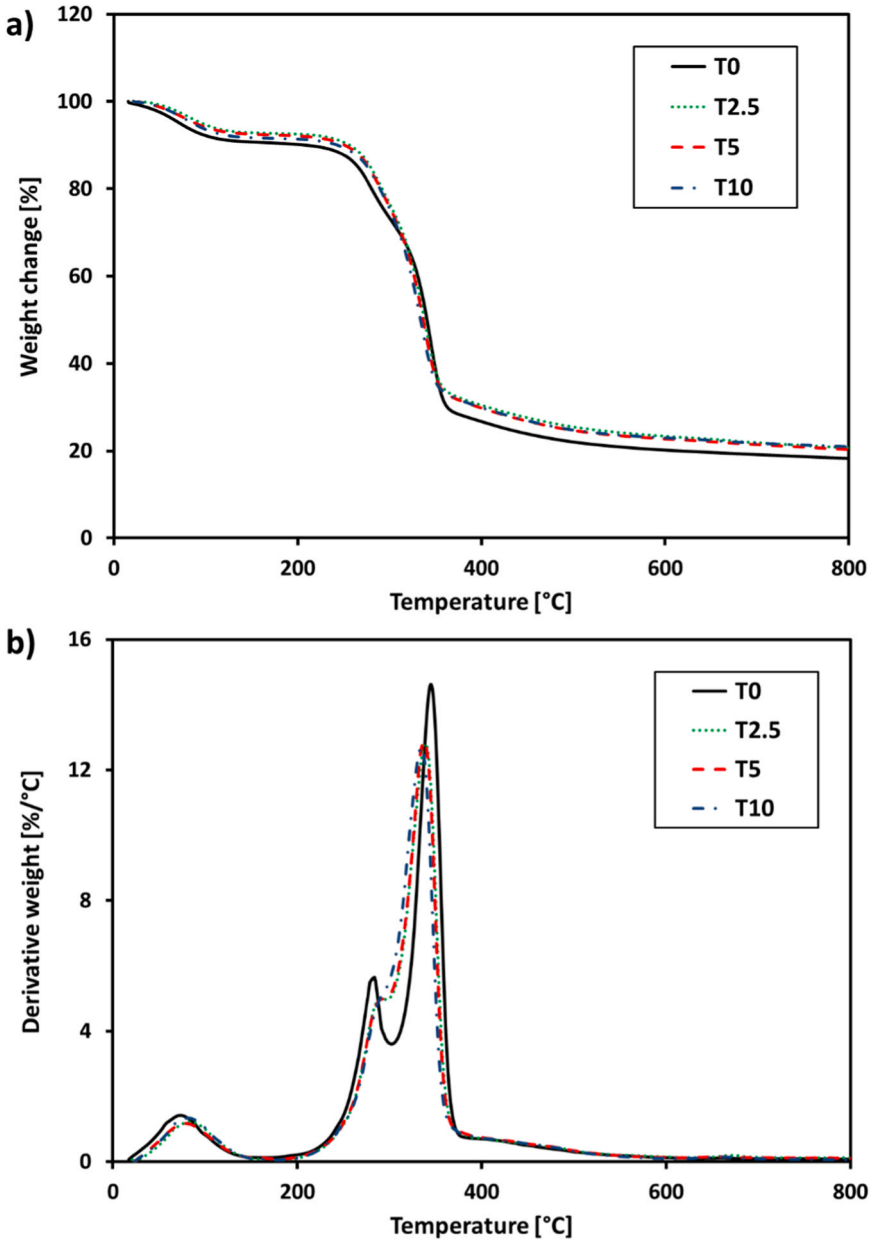

Fig. 8. a) TG and b) DTG curves of untreated and treated sisal fibers.

hemicellulose from sisal fibers. On the other hand, no statement about the lignin reduction can be argued because no peak related to the degradation of this component can be observable from room temperature to 1000 °C.

3.2. Geopolymer composites

The comparison of flexural stress versus strain curves shown by the investigated geopolymer composites is preliminarily reported in Fig. 9.

Overall, the solution concentration (i.e., aggressiveness) led to three main effects on the mechanical behavior of geopolymer composites reinforced with treated sisal fibers:

I. Elastic regime. At low strain values, the linear-elastic zone, strictly correlated to the sample stiffness, slightly increases its slope with increasing the solution aggressiveness. This indicates that the soaking of sisal fibers in sodium bicarbonate positively affects the stiffness of the composite geopolymers;
II. Deflection-hardening regime. At intermediate strain values, the stress versus strain curve partially loses its linear trend after the first-crack triggering in the composite geopolymer. Furthermore, we can observe a monotone trend until the maximum stress value is reached. The addition in the geopolymer composite of treated sisal fibers induces a relevant increase in the maximum strength, which reaches its highest value for MK-T10 samples (i.e., 4.16 MPa, about 2 times higher than that of MK-T0 samples, reinforced with untreated fibers);
III. Deflection-softening regime. Once the maximum stress is reached, a progressive decrease in the composite strength at increasing strain occurs. In particular, the post-peak branch is characterized by a progressive decline in the mechanical stability of all the investigated composites, mainly due to the coalescence and propagation of cracks within the material. It is worth noting that geopolymer composites reinforced with treated fibers (i.e., MK-T2.5, MK-T5 and MK-T10) evidenced by higher stress values in this region as well as less pronounced performances decay, thus indicating better stability to crack propagation in comparison to the untreated sisal fiber reinforced geopolymer (i.e., MK-T0).

According to other literature papers [15,58], the beneficial effects of the fiber treatment on the improved mechanical performances can be attributed to a synergistic action of fiber modification and improved fiber-matrix interfacial adhesion. As widely evidenced through several fiber characterization methods, the mildly alkaline treatment promotes the depletion of hemicellulose and lignin content in sisal fibers, similarly to mercerization [22]. Furthermore, the alkaline treatment increases the surface roughness of sisal fibers, causing their fibrillation. This enhances the interfacial adhesion between the natural fibers and the surrounding geopolymeric matrix, with a similar effect achievable through mercerization [21].

In this context, the inorganic matrix can more easily penetrate and interact with the fiber increasing the mechanical interlocking and the chemical adhesion between these constituents [18]. As a result, beneficial effects on stiffness, strength and post-cracking stability of geopolymer composites were achieved [59]. It important to underline that is behavior may not be considered as predictable by taking into account that sisal fibers progressively modify their morphology after the sodium bicarbonate treatment: i.e., they lose the geometric regularity and structural texture. It was also evidenced that this modification implied the reduction in the tensile strength of the fibers themselves.

However, the mechanical results of geopolymer composites clearly evidenced that the driving force that mainly affects their

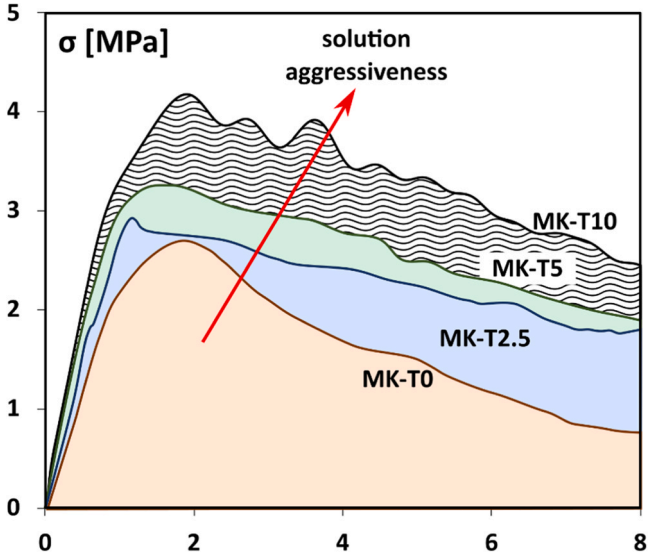

Fig. 9. Typical flexural stress versus strain curves of geopolymer composites.

mechanical performances is the stress transfer ability at the fiber-matrix interface. Consequently, a stronger interfacial bond enhances pull-out resistance and contributes to improved strength and bridging during crack propagation.[60].

From the mechanical point of view, as shown by the stress versus strain curves reported in Fig. 9, the hardening and softening regimes play a key role in amplifying the toughness shown by the composite geopolymers (identifiable as the area under the stress-strain curve).

To this regard, further mechanical features can be identifiable from three-point bending curves in order to better assess the impact of sisal treatment on the toughness of the investigated composites [61].

According to the schematization shown in Fig. 10, it is possible to detect the peak load value (i.e., P_{max}, identified by point A) as well as the load values reached when the sample deflection δ is equal to L/100 (i.e., $P_{L/100}$, point B) and L/40 (i.e., $P_{L/40}$, point C). By considering that the sample length L is equal to 100 mm, the threshold deflection values are equal to 1 mm (point B) and 2.5 mm (point C), respectively. This means that points B and C allow to graphically identify the residual load values suffered by the sample when its deflection is equal to 1 mm and 2.5 mm, respectively. Furthermore, the toughness values related to the same points, defined as $T_{L/100}$ and $T_{L/40}$, can be calculated.

On this regard, Table 3 summarizes the average values and the standard deviation (reported in round brackets) of the main flexural features shown by all the investigated geopolymer composites, both in deflection-hardening and deflection-softening regimes. This table also reports the maximum stress values (σ_{max}) and the related strain ($\varepsilon_{\sigma max}$) when the maximum stress is achieved.

It is worth noting that all load values (i.e., P_{max}, $P_{L/100}$, and $P_{L/40}$) as well as the maximum stress one (i.e., σ_{max}) rise as the solution concentration increases, due to the enhanced capacity to withstand the applied stresses evidenced by treated sisal fibers in comparison to untreated ones. In particular, the high crack-bridging action furnished by treated fibers during the crack opening phase, can be considered as the main key factor to achieve higher load bearing capacity [62].

In particular, the MK-T10 batch exhibited an average peak load value during the deflection-hardening regime equal to 1626 N, i.e., about 600 N higher than that shown by MK-T0. Indeed, geopolymer composites reinforced with sisal fiber treated in low concentrated solutions (i.e., MK-T2.5) show an average P_{max} value equal to 1377, i.e., more than 350 N higher than untreated one (MK-T0). This result confirms the relevant beneficial effect induced by the green surface treatment in the fibers also by using not very aggressive alkaline solution. This large discrepancy between treated and untreated composites is also amplified by evaluating in detail the load deflection-softening regime. By taking into account $P_{L/40}$ as reference parameter, all the treated composites (i.e., MK-2.5, MK-T5 and MK-T10) are characterized by average values more than twice than the MK-T0 batch. Analogous consideration could be argued for $P_{L/100}$ parameter. These results confirm that the fibers surface treatment has also a marked impact in increasing the load bearing capacity of geopolymer composites during the deflection-softening regime. Therefore, the improved fiber homogeneity and interfacial fiber-matrix strength increases the pull-out resistance also enhancing the bridging action offered by short sisal fibers during the crack formation and propagation. The consequence is a significant improve in the energy required to cause the damage evolution and the related collapse of the composite.

On the other hand, both δ_{Pmax} and $\varepsilon_{\sigma max}$ parameters are not clearly dependent on the fiber treatment conditions. Given that these parameters are significantly related to first crack activation in the matrix, they could be more influenced by the mechanical properties of the metakaolin based geopolymer than sisal fibers used as reinforcement [63].

With the aim of better highlighting how the fiber treatment allows to increase the energy required for the damage evolution (Fig. 11). compares the toughness values measured in correspondence of points B and C in Fig. 10 (i.e., $T_{L/100}$ and $T_{L/40}$), at varying the concentration of $NaHCO_3$ solution. The toughness was determined by measuring the area under the load versus deflection curve up to L/100 (i.e., orange diamond markers) and L/40 deflection values (i.e., gray circle markers), respectively.

First of all, it can be noticed that all treated geopolymer composites show higher toughness values than that of the untreated one.

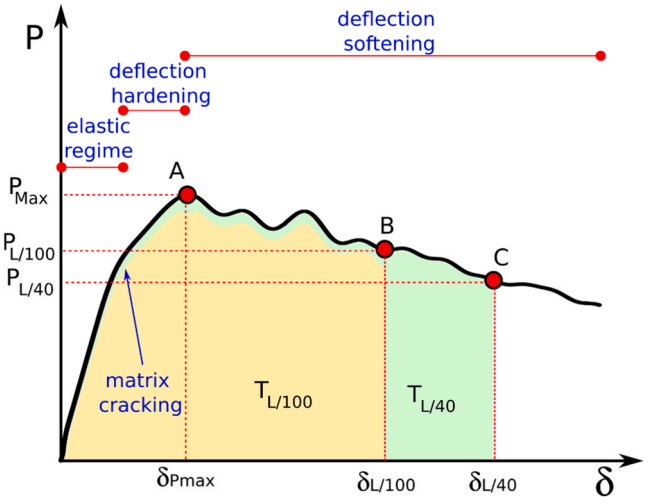

Fig. 10. Schematization of load-deflection curve for a composite geopolymer under three-point bending test.

Table 3
Main features of geopolymer composites subjected to three-point bending test.

	Deflection-Hardening				Deflection-Softening	
	P_{max} [N]	δ_{Pmax} [mm]	σ_{max} [MPa]	$\varepsilon_{\sigma max}$ [%]	$P_{L/100}$ [N]	$P_{L/40}$ [N]
MK-T0	1012	0.68	2.38	1.61	894	465
	(214)	(0.11)	(0.45)	(0.26)	(231)	(103)
MK-T2.5	1377	0.72	3.30	1.71	1339	1009
	(216)	(0.27)	(0.51)	(0.63)	(214)	(197)
MK-T5	1477	0.59	3.48	1.41	1360	958
	(117)	(0.13)	(0.30)	(0.31)	(141)	(137)
MK-T10	1626	0.83	3.92	1.98	1532	1141
	(255)	(0.08)	(0.63)	(0.20)	(181)	(127)

* the standard deviation in round brackets

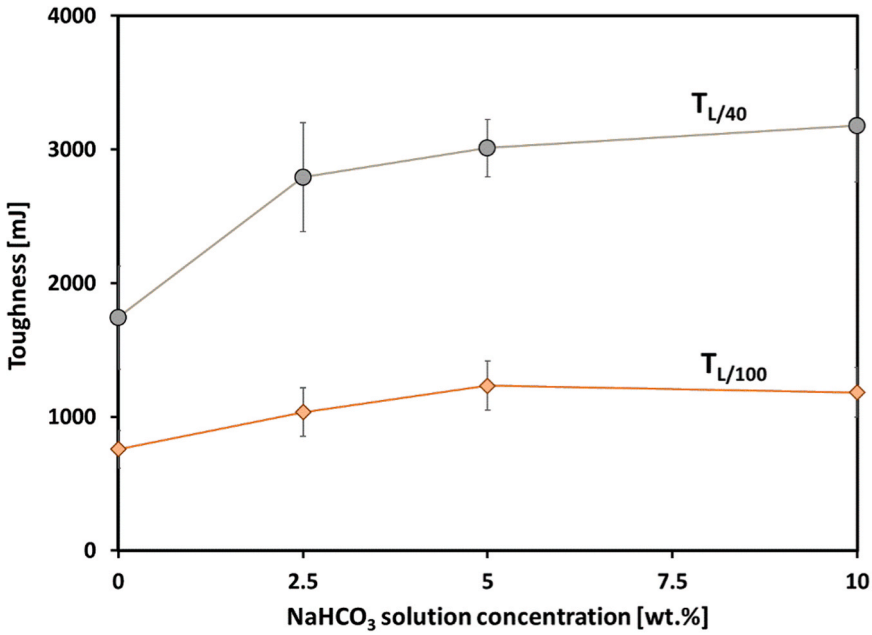

Fig. 11. Evolution of geopolymer composites toughness values measured at specified L/100 and L/40 deflections.

Furthermore, both parameters exhibit a distinct monotone trend. In particular, a $NaHCO_3$ concentration equal to 10 wt% resulted in $T_{L/100}$ and $T_{L/40}$ values which are about 55 % and 80 % greater than those of MK-T0 composite, respectively. In the deflection-hardening and deflection-softening regimes, the flexural features of geopolymer composites are greatly affected by the role against the crack propagation played by treated sisal fibers [64].

As widely demonstrated, the $NaHCO_3$ based treatment is able to remove impurities and waxy substances from the fiber surface, thus exposing more active sites for bonding with the surrounding geopolymer matrix [22,27]. At the same time, the treatment partially removes hemicellulose that can act as stress concentrators, being an amorphous polysaccharide promoting defects in the fiber structure [65,66]. All these effects greatly contribute to the enhancement of fiber-matrix adhesion, thus leading to more effective stress transfer between them and, as a consequence, resulting in improved composite strength and toughness. In this regard, the increase of the surface roughness of the fiber also impacts beneficially on the mechanical performance of the geopolymer composites. In particular, it promotes the mechanical interlocking between sisal fibers and matrix, further enhancing the composites' resistance to crack propagation in addition to improving their overall toughness [67].

The improved mechanical properties (i.e., particularly the enhanced toughness) shown by geopolymers reinforced with sisal fibers previously treated through sodium bicarbonate solution, prove that this eco-friendly treatment represents an effective approach to develop high-performance composites for a variety of applications in the construction field. The enhanced toughness and strength of these composites suggest their suitability for use in structural components, building panels, and other demanding applications where durability and resilience are crucial.

4. Conclusion

The study investigated the effects of a mild alkaline treatment using sodium bicarbonate ($NaHCO_3$) on the surface chemistry, morphology, mechanical properties, and thermal stability of sisal fibers. The treated fibers were then incorporated into geopolymer composites to evaluate the improvement in their mechanical performance. The main findings can be identified in:

- Fiber Treatment: The $NaHCO_3$ treatment effectively removed hemicellulose and partially removed lignin and waxes from the sisal fiber surface. This treatment increased the surface roughness and induced fiber fibrillation, enhancing the potential for better bonding with the geopolymer matrix.
- Fiber Properties: Although the treatment improved the interfacial bonding potential, it also slightly decreased the tensile strength of the treated fibers compared to the untreated ones.
- Geopolymer Composites: The geopolymer composites reinforced with treated sisal fibers exhibited an improved of 53 % in flexural strength and 82 % in toughness compared to the composites with untreated fibers. This improvement is attributed to the enhanced fiber-matrix interfacial adhesion due to the surface modifications of the treated fibers.
- Treatment Optimization: While a low concentration might not be aggressive enough to achieve significant surface modification, a very high concentration could lead to excessive fiber degradation and compromise its mechanical properties. Thus, an optimal weight concentration of 10 % for the $NaHCO_3$ solution was identified.

Overall, the study demonstrates that a mild alkaline treatment with $NaHCO_3$ can be a viable approach to improve the interfacial bonding between sisal fibers and geopolymer matrices, leading to enhanced mechanical and toughness performance of the resulting composites.

Declaration of Competing Interest

The authors declare that they have no known competing financial interests or personal relationships that could have appeared to influence the work reported in this paper.

Data availability

Data will be made available on request.

Acknowledgments

The authors thank Chiraema s.r.l. for supplying the metakaolin.

References

[1] N. Ranjbar, M. Zhang, Fiber-reinforced geopolymer composites: a review, Cem. Concr. Compos. 107 (2020), https://doi.org/10.1016/j.cemconcomp.2019.103498.
[2] M.M. Camargo, E. Adefrs Taye, J.A. Roether, D. Tilahun Redda, A.R. Boccaccini, A review on natural fiber-reinforced geopolymer and cement-based composites, Materials 13 (2020), https://doi.org/10.3390/ma13204603.
[3] B. Majidi, Geopolymer technology, from fundamentals to advanced applications: a review, Mater. Technol. 24 (2009) 79–87, https://doi.org/10.1179/175355509X449355.
[4] S. T, K.R. P.R, S. M, S. A, J. R, A state-of-the-art on development of geopolymer concrete and its field applications, Case Stud. Constr. Mater. 16 (2022) e00812, https://doi.org/10.1016/j.cscm.2021.e00812.
[5] A.R.G. de Azevedo, A.S.A. Cruz, M.T. Marvila, L.B. de Oliveira, S.N. Monteiro, C.M.F. Vieira, R. Fediuk, R. Timokhin, N. Vatin, M. Daironas, Natural fibers as an alternative to synthetic fibers in reinforcement of geopolymer matrices: a comparative review, Polymers 13 (2021), https://doi.org/10.3390/polym13152493.
[6] E. Haily, N. Zari, R. Bouhfid, A. Qaiss, Natural fibers as an alternative to synthetic fibers in the reinforcement of phosphate sludge-based geopolymer mortar, J. Build. Eng. 67 (2023) 105947, https://doi.org/10.1016/j.jobe.2023.105947.
[7] G. Silva, S. Kim, R. Aguilar, J. Nakamatsu, Natural fibers as reinforcement additives for geopolymers – a review of potential eco-friendly applications to the construction industry, Sustain. Mater. Technol. 23 (2020) e00132, https://doi.org/10.1016/j.susmat.2019.e00132.
[8] K.Z. Farhan, M.A.M. Johari, R. Demirboğa, Impact of fiber reinforcements on properties of geopolymer composites: a review, J. Build. Eng. 44 (2021) 102628, https://doi.org/10.1016/j.jobe.2021.102628.
[9] C. Rahmawati, S. Aprilia, T. Saidi, T.B. Aulia, A. Amin, J. Ahmad, H.F. Isleem, Mechanical properties and fracture parameters of geopolymers based on cellulose nanocrystals from Typha sp. fibers, Case Stud. Constr. Mater. 17 (2022) e01498, https://doi.org/10.1016/j.cscm.2022.e01498.
[10] L. Calabrese, V. Fiore, E. Piperopoulos, D. Badagliacco, D. Palamara, A. Valenza, E. Proverbio, In situ monitoring of moisture uptake of flax fiber reinforced composites under humid/dry conditions, J. Appl. Polym. Sci. 139 (2022) 51969, https://doi.org/10.1002/app.51969.
[11] J.A. Halip, L.S. Hua, Z. Ashaari, P.M. Tahir, L.W. Chen, M.K. Anwar Uyup, 8 - Effect of treatment on water absorption behavior of natural fiber–reinforced polymer composites, in: M. Jawaid, M. Thariq, N.B.T.-M. and P.T. of B. Saba Fibre-Reinforced Composites and Hybrid Composites (Eds.), Woodhead Publ. Ser. Compos. Sci. Eng., Woodhead Publishing, 2019: pp. 141–156. https://doi.org/https://doi.org/10.1016/B978-0-08-102292-4.00008-4. .
[12] T.R. da Silva, P.R. de Matos, L.U.D. Tambara Júnior, M.T. Marvila, A.R.G. de Azevedo, A review on the performance of açaí fiber in cementitious composites: characteristics and application challenges, J. Build. Eng. 71 (2023) 106481, https://doi.org/10.1016/j.jobe.2023.106481.
[13] M.G. Veigas, M. Najimi, B. Shafei, Cementitious composites made with natural fibers: Investigation of uncoated and coated sisal fibers, Case Stud. Constr. Mater. 16 (2022) e00788, https://doi.org/10.1016/j.cscm.2021.e00788.
[14] T. Suwan, P. Maichin, M. Fan, P. Jitsangiam, W. Tangchirapat, P. Chindaprasirt, Influence of alkalinity on self-treatment process of natural fiber and properties of its geopolymeric composites, Constr. Build. Mater. 316 (2022), https://doi.org/10.1016/j.conbuildmat.2021.125817.
[15] R.A.J. Malenab, J.P.S. Ngo, M.A.B. Promentilla, Chemical treatment of waste abaca for natural fiber-reinforced geopolymer composite, Materials 10 (2017), https://doi.org/10.3390/ma10060579.

[16] B. Koohestani, A.K. Darban, P. Mokhtari, E. Yilmaz, E. Darezereshki, Comparison of different natural fiber treatments: a literature review, Int. J. Environ. Sci. Technol. 16 (2019) 629–642, https://doi.org/10.1007/s13762-018-1890-9.
[17] J.S.S. Neto, R.A.A. Lima, D.K.K. Cavalcanti, J.P.B. Souza, R.A.A. Aguiar, M.D. Banea, Effect of chemical treatment on the thermal properties of hybrid natural fiber-reinforced composites, J. Appl. Polym. Sci. 136 (2019) 47154, https://doi.org/10.1002/app.47154.
[18] K. Sankar, A.C. Constâncio Trindade, W.M. Kriven, The influence of alkaline treatment on the mechanical performance of geopolymer composites reinforced with Brazilian malva and curaua fibers, J. Am. Ceram. Soc. 106 (2023) 339–353, https://doi.org/10.1111/jace.18716.
[19] K.M.F. Hasan, P.G. Horváth, T. Alpár, Lignocellulosic fiber cement compatibility: a state of the art review, J. Nat. Fibers 19 (2022) 5409–5434, https://doi.org/10.1080/15440478.2021.1875380.
[20] M.G. Sá Ribeiro, I.P.A. Miranda, W.M. Kriven, A. Ozer, R.A. Sá Ribeiro, High strength and low water absorption of bamboo fiber-reinforced geopolymer composites, Constr. Build. Mater. 411 (2024) 134179, https://doi.org/10.1016/j.conbuildmat.2023.134179.
[21] G. Lazorenko, A. Kasprzhitskii, V. Yavna, V. Mischinenko, A. Kukharskii, A. Kruglikov, A. Kolodina, G. Yalovega, Effect of pre-treatment of flax tows on mechanical properties and microstructure of natural fiber reinforced geopolymer composites, Environ. Technol. Innov. 20 (2020), https://doi.org/10.1016/j.eti.2020.101105.
[22] V. Fiore, T. Scalici, F. Nicoletti, G. Vitale, M. Prestipino, A. Valenza, A new eco-friendly chemical treatment of natural fibres: effect of sodium bicarbonate on properties of sisal fibre and its epoxy composites, Compos. Part B Eng. 85 (2016) 150–160, https://doi.org/10.1016/j.compositesb.2015.09.028.
[23] J.C. dos Santos, R.L. Siqueira, L.M.G. Vieira, R.T.S. Freire, V. Mano, T.H. Panzera, Effects of sodium carbonate on the performance of epoxy and polyester coir-reinforced composites, Polym. Test. 67 (2018) 533–544, https://doi.org/10.1016/j.polymertesting.2018.03.043.
[24] S. Chaitanya, I. Singh, Sisal fiber-reinforced green composites: effect of ecofriendly fiber treatment, Polym. Compos. 39 (2018) 4310–4321, https://doi.org/10.1002/pc.24511.
[25] V. Fiore, T. Scalici, A. Valenza, Effect of sodium bicarbonate treatment on mechanical properties of flax-reinforced epoxy composite materials, J. Compos. Mater. 52 (2018) 1061–1072, https://doi.org/10.1177/0021998317720009.
[26] V. Fiore, C. Sanfilippo, L. Calabrese, Influence of sodium bicarbonate treatment on the aging resistance of natural fiber reinforced polymer composites under marine environment, Polym. Test. 80 (2019) 106100, https://doi.org/10.1016/j.polymertesting.2019.106100.
[27] J.C. Dos Santos, P.R. Oliveira, R.T.S. Freire, L.M.G. Vieira, J.C.C. Rubio, T.H. Panzera, The effects of sodium carbonate and bicarbonate treatments on sisal fibre composites, Mater. Res. 25 (2022), https://doi.org/10.1590/1980-5373-MR-2021-0464.
[28] A. Belaadi, S. Amroune, M. Bourchak, Effect of eco-friendly chemical sodium bicarbonate treatment on the mechanical properties of flax fibres: Weibull statistics, Int. J. Adv. Manuf. Technol. 106 (2019) 1753–1774, https://doi.org/10.1007/s00170-019-04628-8.
[29] J. Zamboni Schiavon, J.J. de Oliveira Andrade, Comparison between alternative chemical treatments on coir fibers for application in cementitious materials, J. Mater. Res. Technol. 25 (2023) 4634–4649, https://doi.org/10.1016/j.jmrt.2023.06.210.
[30] J.Z. Schiavon, P.M. Borges, J.J. de Oliveira Andrade, Physical-mechanical properties and microstructure changes in mortars with chemically treated coir fibers, J. Mater. Res. Technol. 30 (2024) 4030–4043, https://doi.org/10.1016/j.jmrt.2024.04.109.
[31] I. Mukhtar, Z. Leman, E.S. Zainudin, M.R. Ishak, Effectiveness of alkali and sodium bicarbonate treatments on sugar palm fiber: mechanical, thermal, and chemical investigations, J. Nat. Fibers (2018) 1–13, https://doi.org/10.1080/15440478.2018.1537872.
[32] Y. Seki, M. Sarikanat, K. Sever, C. Durmuşkahya, Extraction and properties of Ferula communis (chakshir) fibers as novel reinforcement for composites materials, Compos. Part B Eng. 44 (2013) 517–523, https://doi.org/10.1016/j.compositesb.2012.03.013.
[33] S. Amroune, A. Bezazi, A. Dufresne, F. Scarpa, A. Imad, Investigation of the date palm fiber for green composites reinforcement: thermo-physical and mechanical properties of the fiber, J. Nat. Fibers 18 (2021) 717–734, https://doi.org/10.1080/15440478.2019.1645791.
[34] A. Alawar, A.M. Hamed, K. Al-Kaabi, Characterization of treated date palm tree fiber as composite reinforcement, Compos. Part B Eng. 40 (2009) 601–606, https://doi.org/10.1016/j.compositesb.2009.04.018.
[35] P. Maichin, T. Suwan, P. Jitsangiam, P. Chindaprasirt, M. Fan, Effect of self-treatment process on properties of natural fiber-reinforced geopolymer composites, Mater. Manuf. Process. 35 (2020) 1120–1128, https://doi.org/10.1080/10426914.2020.1767294.
[36] A. El Oudiani, S. Msahli, F. Sakli, In-depth study of agave fiber structure using Fourier transform infrared spectroscopy, Carbohydr. Polym. 164 (2017) 242–248, https://doi.org/10.1016/j.carbpol.2017.01.091.
[37] A. Kumar, B. Biswas, K. Saini, A. Kumar, J. Kumar, B.B. Krishna, T. Bhaskar, Effect of hydrogen peroxide on the depolymerization of prot lignin, Ind. Crops Prod. 150 (2020) 112355, https://doi.org/10.1016/j.indcrop.2020.112355.
[38] X. Liu, C.M.G.C. Renard, S. Bureau, C. Le Bourvellec, Revisiting the contribution of ATR-FTIR spectroscopy to characterize plant cell wall polysaccharides, Carbohydr. Polym. 262 (2021) 117935, https://doi.org/10.1016/j.carbpol.2021.117935.
[39] M. Le Troedec, D. Sedan, C. Peyratout, J.P. Bonnet, A. Smith, R. Guinebretiere, V. Gloaguen, P. Krausz, Influence of various chemical treatments on the composition and structure of hemp fibres, Compos. Part A Appl. Sci. Manuf. 39 (2008) 514–522, https://doi.org/10.1016/j.compositesa.2007.12.001.
[40] R. Md Salim, J. Asik, M.S. Sarjadi, Chemical functional groups of extractives, cellulose and lignin extracted from native Leucaena leucocephala bark, Wood Sci. Technol. 55 (2021) 295–313, https://doi.org/10.1007/s00226-020-01258-2.
[41] J. Liang, Y. Zeng, H. Wang, W. Lou, Extraction, purification and antioxidant activity of novel polysaccharides from Dendrobium officinale by deep eutectic solvents, Nat. Prod. Res. 33 (2019) 3248–3253, https://doi.org/10.1080/14786419.2018.1471480.
[42] M.C. Paiva, I. Ammar, A.R. Campos, R.B. Cheikh, A.M. Cunha, Alfa fibres: Mechanical, morphological and interfacial characterization, Compos. Sci. Technol. 67 (2007) 1132–1138, https://doi.org/10.1016/j.compscitech.2006.05.019.
[43] Y. Seki, S. Köktaş, A.Ç. Kılınç, R. Dalmis, Green alternative treatment for cellulosic fibers: ionic liquid modification of Abelmoschus esculentus fibers with methyl-tri-n-butyl ammonium methyl sulphate, Mater. Res. Express 6 (2019) 85104, https://doi.org/10.1088/2053-1591/ab2015.
[44] J.C. dos Santos, L.Á. de Oliveira, L.M. Gomes Vieira, V. Mano, R.T.S. Freire, T.H. Panzera, Eco-friendly sodium bicarbonate treatment and its effect on epoxy and polyester coir fibre composites, Constr. Build. Mater. 211 (2019) 427–436, https://doi.org/10.1016/j.conbuildmat.2019.03.284.
[45] A. Vinod, M.R. Sanjay, S. Suchart, P. Jyotishkumar, Renewable and sustainable biobased materials: an assessment on biofibers, biofilms, biopolymers and biocomposites, J. Clean. Prod. 258 (2020), https://doi.org/10.1016/j.jclepro.2020.120978.
[46] K.S. Chun, T. Maimunah, C.M. Yeng, T.K. Yeow, O.T. Kiat, Properties of corn husk fibre reinforced epoxy composites fabricated using vacuum-assisted resin infusion, J. Phys. Sci. 31 (2020) 17–31, https://doi.org/10.21315/jps2020.31.3.2.
[47] J.C. dos Santos, R.L. Siqueira, L.M.G. Vieira, R.T.S. Freire, V. Mano, T.H. Panzera, Effects of sodium carbonate on the performance of epoxy and polyester coir-reinforced composites, Polym. Test. 67 (2018) 533–544, https://doi.org/10.1016/j.polymertesting.2018.03.043.
[48] M.F. Taimur-Al-Mobarak, M.A. Mina, A.N. Gafur, S.A. Ahmed, Dhar, Effect of chemical modifications on surface morphological, structural, mechanical, and thermal properties of sponge-gourd natural fiber, Fibers Polym. 19 (2018) 31–40, https://doi.org/10.1007/s12221-018-7199-3.
[49] S. Ouajai, R.A. ShanksComposition, structure and thermal degradation of hemp cellulose after chemical treatments, 89 (2005) 327–335. https://doi.org/10.1016/j.polymdegradstab.2005.01.016. .
[50] C.H. Lee, A. Khalina, S.H. Lee, Importance of interfacial adhesion condition on characterization of plant-fiber-reinforced polymer composites: a review, Polymers 13 (2021) 438, https://doi.org/10.3390/polym13030438.
[51] J. Wei, C. Meyer, Degradation mechanisms of natural fiber in the matrix of cement composites, Cem. Concr. Res. 73 (2015) 1–16, https://doi.org/10.1016/j.cemconres.2015.02.019.
[52] C. Lv, J. Liu, Alkaline degradation of plant fiber reinforcements in geopolymer: a review, Molecules 28 (2023), https://doi.org/10.3390/molecules28041868.
[53] T.H. Nam, S. Ogihara, N.H. Tung, S. Kobayashi, Effect of alkali treatment on interfacial and mechanical properties of coir fiber reinforced poly(butylene succinate) biodegradable composites, Compos. Part B Eng. 42 (2011) 1648–1656, https://doi.org/10.1016/j.compositesb.2011.04.001.
[54] P. Manimaran, S.P. Saravanan, M.R. Sanjay, M. Jawaid, S. Siengchin, V. Fiore, New lignocellulosic aristida adscensionis fibers as novel reinforcement for composite materials: extraction, characterization and weibull distribution analysis, J. Polym. Environ. 28 (2020) 803–811, https://doi.org/10.1007/s10924-019-01640-7.

[55] V. Fiore, D. Badagliacco, C. Sanfilippo, R. Pirrone, S. Siengchin, S.M. Rangappa, L. Botta, Lemongrass plant as potential sources of reinforcement for biocomposites: a preliminary experimental comparison between leaf and culm fibers, J. Polym. Environ. 30 (2022) 4726–4737, https://doi.org/10.1007/s10924-022-02545-8.
[56] R.M. Luqman, M. Azlan Suhot, M. Zaki Hassan, Effect of alkaline treatment on the single natural fiber strength using Weibull analysis probabilistic model, Mater. Today Proc. (2023), https://doi.org/10.1016/j.matpr.2023.01.108.
[57] I.M. De Rosa, J.M. Kenny, D. Puglia, C. Santulli, F. Sarasini, Morphological, thermal and mechanical characterization of okra (Abelmoschus esculentus) fibres as potential reinforcement in polymer composites, Compos. Sci. Technol. 70 (2010) 116–122, https://doi.org/10.1016/j.compscitech.2009.09.013.
[58] R. Chen, S. Ahmari, L. Zhang, Utilization of sweet sorghum fiber to reinforce fly ash-based geopolymer, J. Mater. Sci. 49 (2014) 2548–2558, https://doi.org/10.1007/s10853-013-7950-0.
[59] S. Cui, Y. Sheng, Z. Wang, H. Jia, W. Qiu, A. Abdulakeem Temitope, Z. Xu, Effect of the fiber surface treatment on the mechanical performance of bamboo fiber modified asphalt binder, Constr. Build. Mater. 347 (2022) 128453, https://doi.org/10.1016/j.conbuildmat.2022.128453.
[60] M.D. de Klerk, M. Kayondo, G.M. Moelich, W.I. de Villiers, R. Combrinck, W.P. Boshoff, Durability of chemically modified sisal fibre in cement-based composites, Constr. Build. Mater. 241 (2020) 117835, https://doi.org/10.1016/j.conbuildmat.2019.117835.
[61] G. Gullì, R. Bertino, F. Grungo, D. Palamara, P. Bruzzaniti, L. Calabrese, Flexural toughening of hooked-end steel fibers reinforced mortars, Appl. Sci. Eng. Prog. 17 (2024) 7030, https://doi.org/10.14416/j.asep.2023.11.004.
[62] G. Gullì, D. Palamara, P. Bruzzaniti, R. Bertino, F. Grungo, L. Calabrese, Flexural toughening of a cementitious mortar reinforced with wave-shaped short plastic fibers, JOM 75 (2023) 537–548, https://doi.org/10.1007/s11837-022-05623-3.
[63] G. Yazıcı, V. İnan, Tabak, Effect of aspect ratio and volume fraction of steel fiber on the mechanical properties of SFRC, Constr. Build. Mater. 21 (2007) 1250–1253, https://doi.org/10.1016/j.conbuildmat.2006.05.025.
[64] Y. Ding, Y.-L. Bai, Fracture properties and softening curves of steel fiber-reinforced slag-based geopolymer mortar and concrete, Materials 11 (2018), https://doi.org/10.3390/ma11081445.
[65] A. Bourmaud, H. Dhakal, A. Habrant, J. Padovani, D. Siniscalco, M.H. Ramage, J. Beaugrand, D.U. Shah, Exploring the potential of waste leaf sheath date palm fibres for composite reinforcement through a structural and mechanical analysis, Compos. Part A Appl. Sci. Manuf. 103 (2017) 292–303, https://doi.org/10.1016/j.compositesa.2017.10.017.
[66] M. Cai, H. Takagi, A.N. Nakagaito, M. Katoh, T. Ueki, G.I.N. Waterhouse, Y. Li, Influence of alkali treatment on internal microstructure and tensile properties of abaca fibers, Ind. Crops Prod. 65 (2015) 27–35, https://doi.org/10.1016/j.indcrop.2014.11.048.
[67] O. Laban, E. Mahdi, Enhancing mode I inter-laminar fracture toughness of aluminum/fiberglass fiber-metal laminates by combining surface pre-treatments, Int. J. Adhes. Adhes. 78 (2017) 234–239, https://doi.org/10.1016/j.ijadhadh.2017.08.008.